Supporting Information

Multilayer Hierarchical Interfaces with High Energy Density in Polymer Nanocomposites Composed of $BaTiO_3@TiO_2@Al_2O_3$ Nanofibers

Zhongbin Pan[a], Jiwei Zhai[a*], and Bo Shen[a]

[a]Key Laboratory of Advanced Civil Engineering Materials, Ministry of Education, School of Materials Science & Engineering, Tongji University, 4800 Caoan Road, Shanghai 201804, China.

[*]E-mail: apzhai@tongji.edu.cn (Jiwei Zhai)

Supporting Information 1

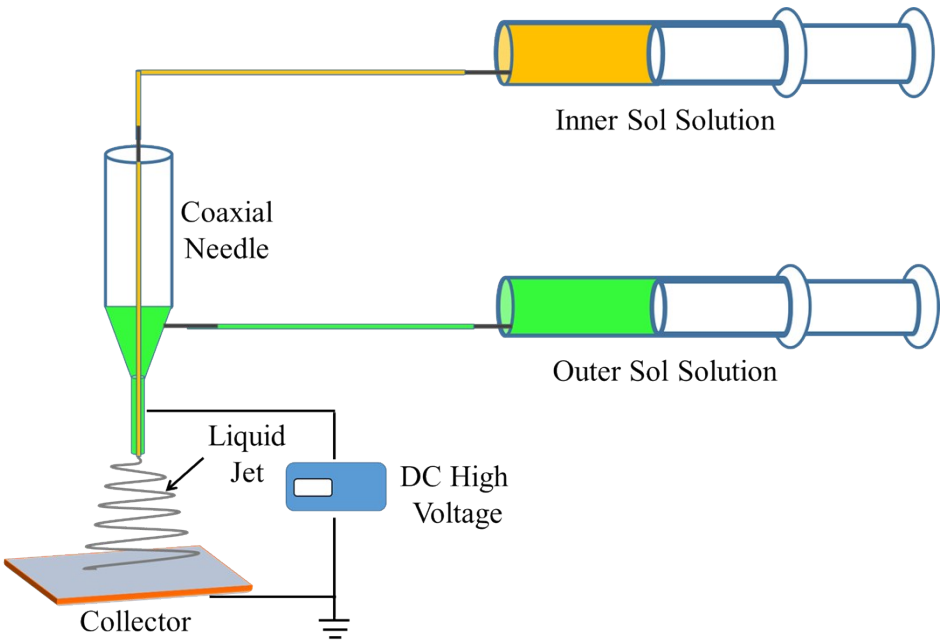

Figure S1 Schematic of the coaxial electrospinning.

Supporting Information 2

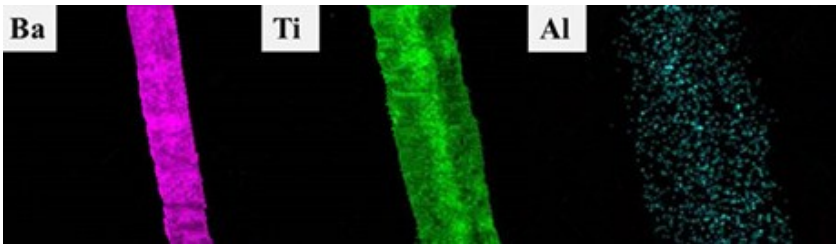

Figure S2 Element mapping images of Ba, Ti, and Al for the BT@TO@AO NFs.

Supporting Information 3

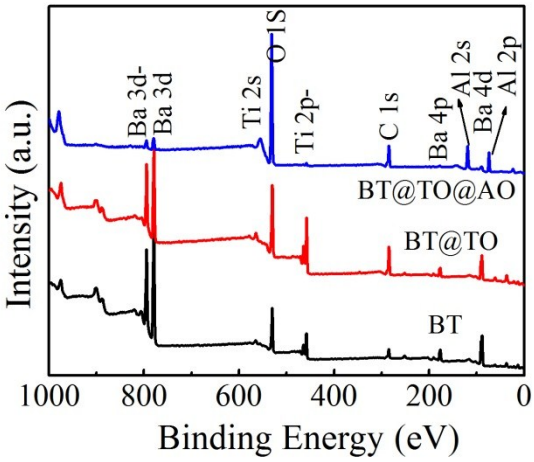

Figure S3 XPS of BT NFs, BT@TO NFs and BT@TO@AO NFs.

Compared with the BT NFs, the peak intensity of O 1s and Ti 2p^{-} of BT@TO NFs become more and more high, which comes from the TO. New peak of Al 2s and Al 2p could be observed in the BT@TO@AO NFs, Which provides by AO. In addition, the peak intensity of O 1s become also high, which originates from the TO and AO. These results further reveal that the BT@TO@AO NFs have been successfully prepared.

Supporting Information 4

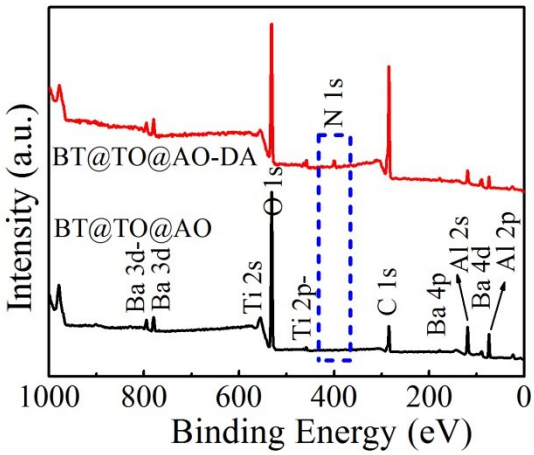

Figure S4 XPS of the BT@TO@AO NFs and BT@TO@AO NFs-DA.

The additional peak of N 1s in BT@TO@AO -DA NFs appears at approximately 401 eV, which is ascribed to the free amino group, indicating the successful incorporation of dopamine onto the BT@TO@AO NFs surfaces.

Supporting Information 5

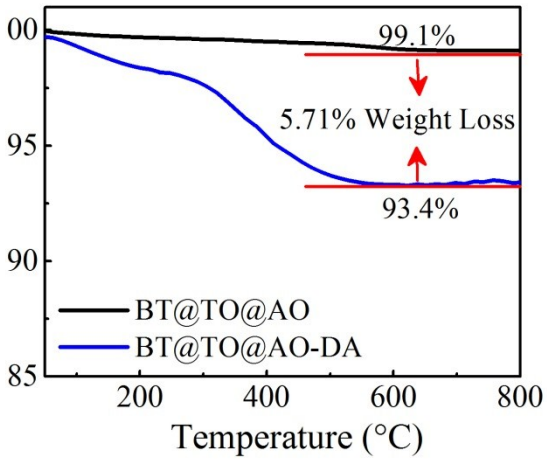

Figure S5 TG curves the BT@TO@AO NFs and BT@TO@AO NFs-DA.

Supporting Information 6

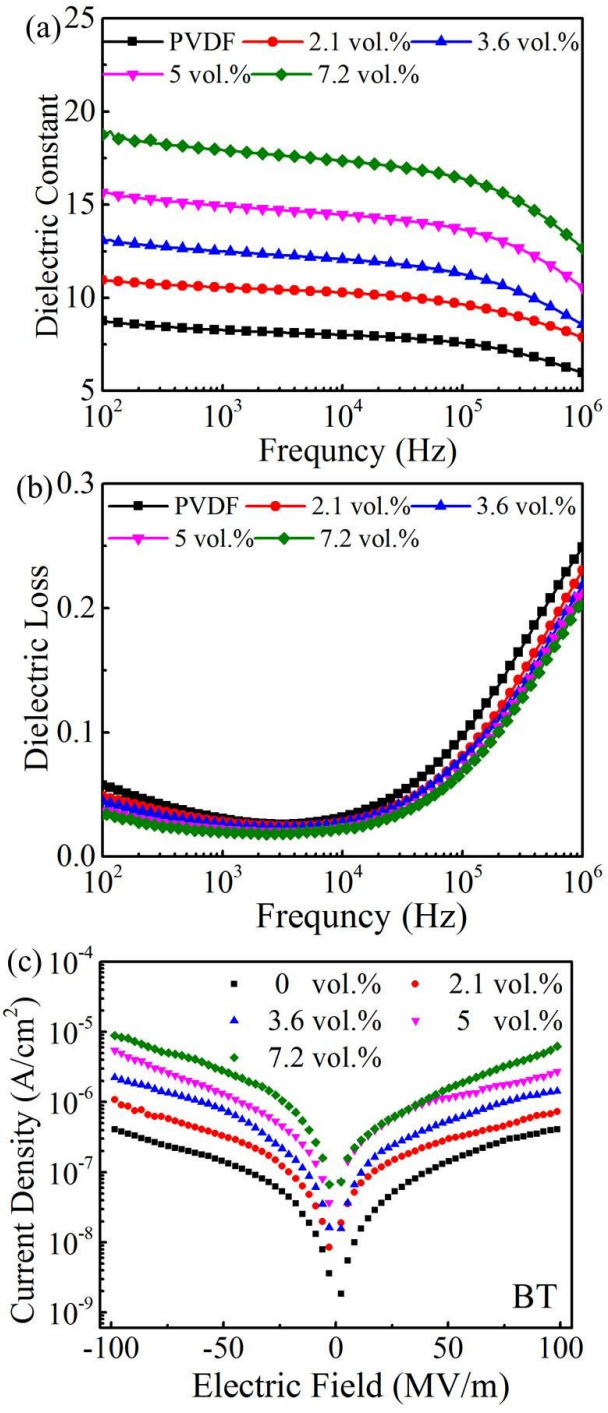

Figure S6 Frequency dependence of dielectric constant (a) dielectric loss (b), and electric field dependence of the current density (c) of the BT NFs/PVDF nanocomposites.

Supporting Information 7

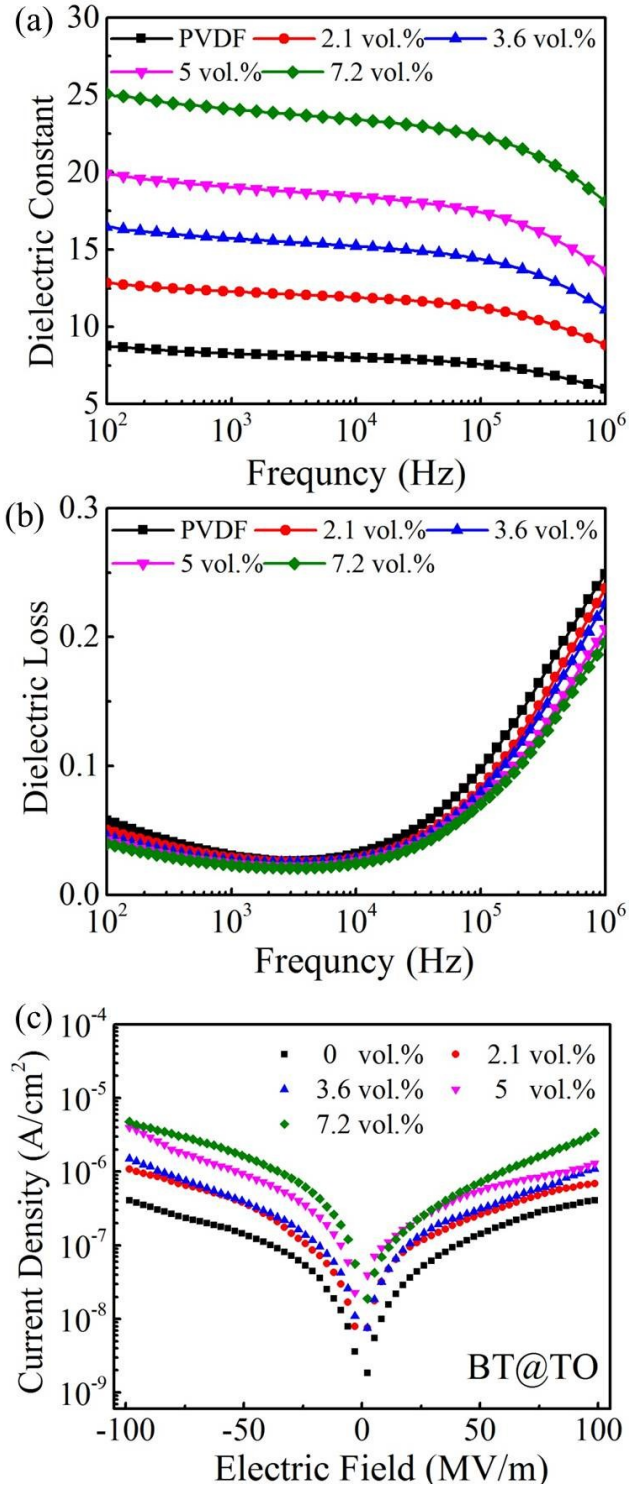

Figure S7 Frequency dependence of dielectric constant (a) dielectric loss (b), and electric field dependence of the current density (c) of the BT@TO NFs/PVDF

nanocomposites.

Supporting Information 8

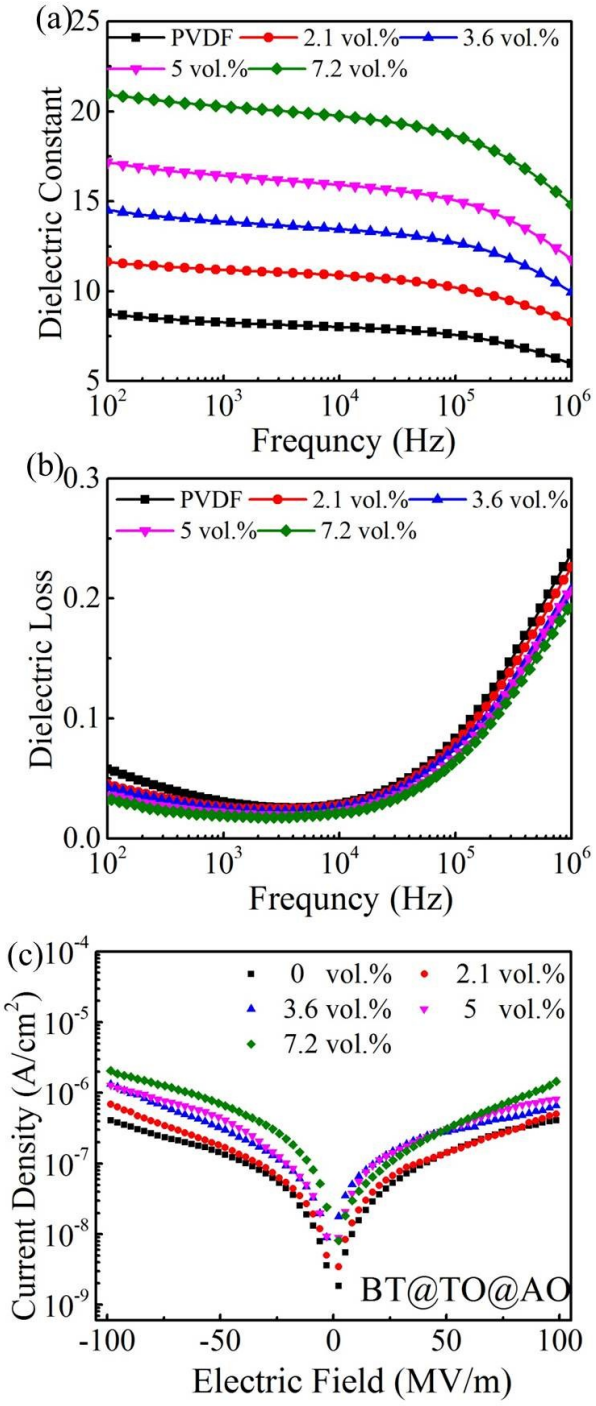

Figure S8 Frequency dependence of dielectric constant (a) dielectric loss (b), and electric field dependence of the current density (c) of the BT@TO@AO NFs/PVDF nanocomposites.

Supporting Information 9

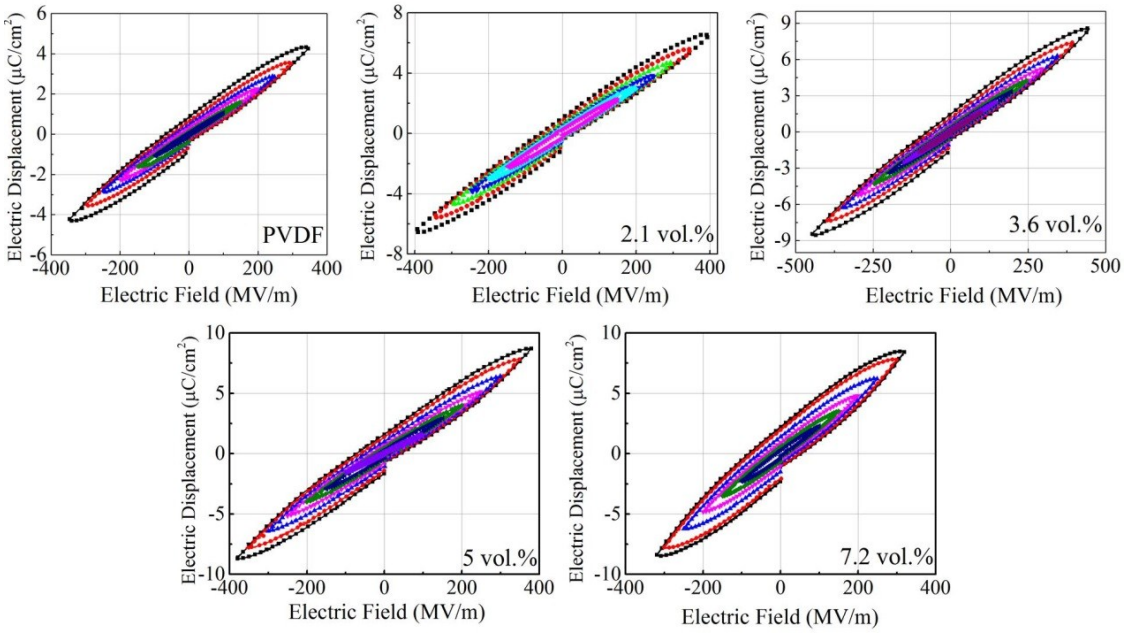

Figure S9 D-E loops of nanocomposites loaded with different contents of BT@TO@AO NFs.

Supporting Information 10

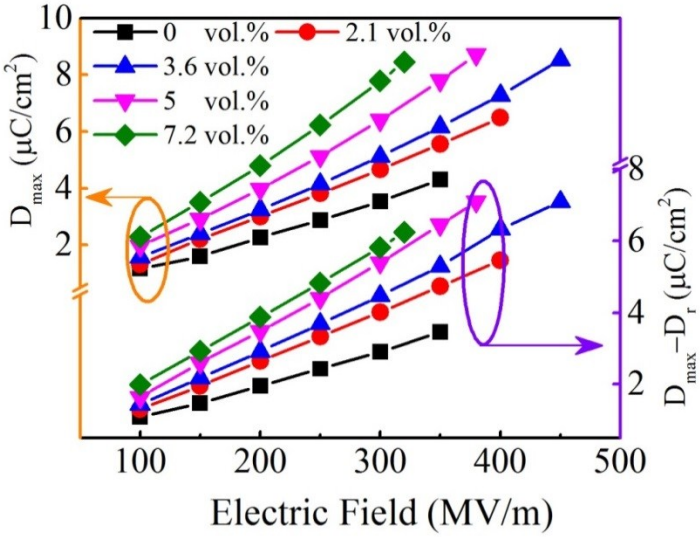

Figure S10 Electric field dependence of Maximum polarization and Maximum polarization – remnant polarization of nanocomposites loaded with different contents

of BT@TO@AO NFs.

Supporting Information 11

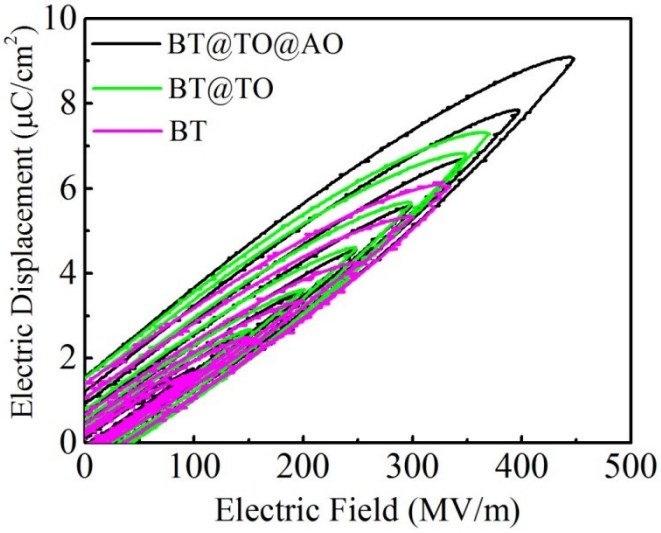

Figure S11 D-E curves of nanocompoaites loaded with 3.6 % BT NFs, BT@TO NFs, and BT@TO@AO NFs.

Supporting Information 12

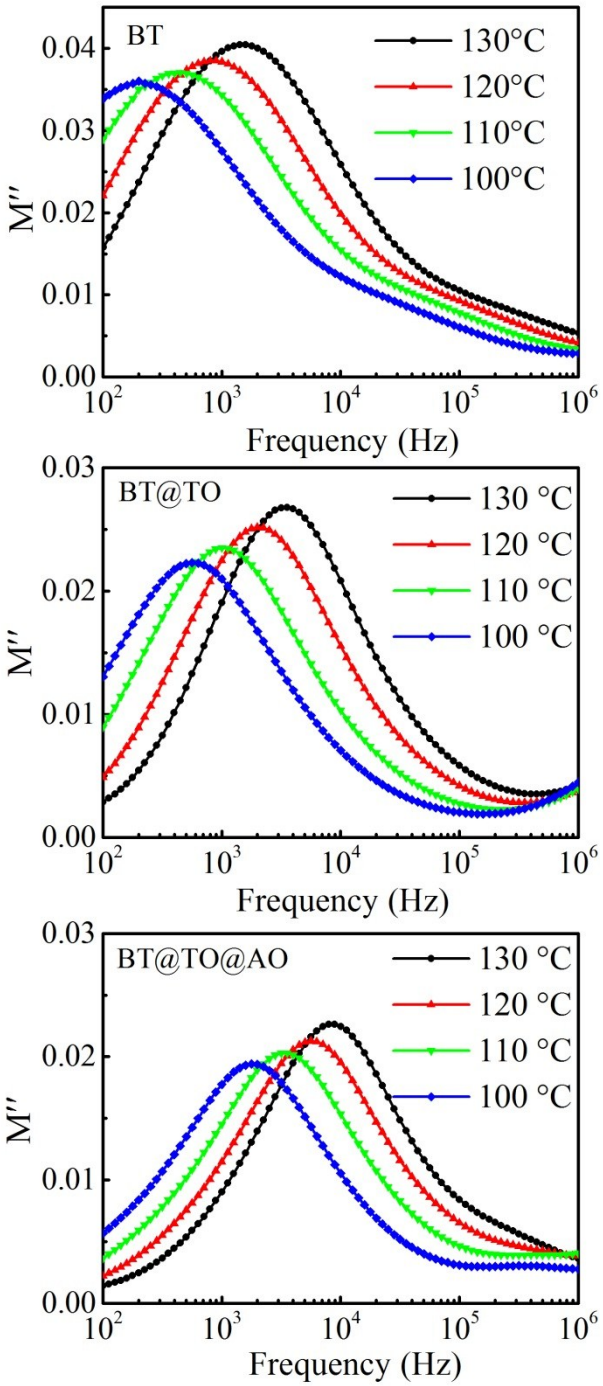

Figure S12 Frequency dependence of imaginary electric modulus (M") of nanocompoaites loaded with 3.6 % BT NFs, BT@TO NFs, and BT@TO@AO NFs.

Supporting Information 13

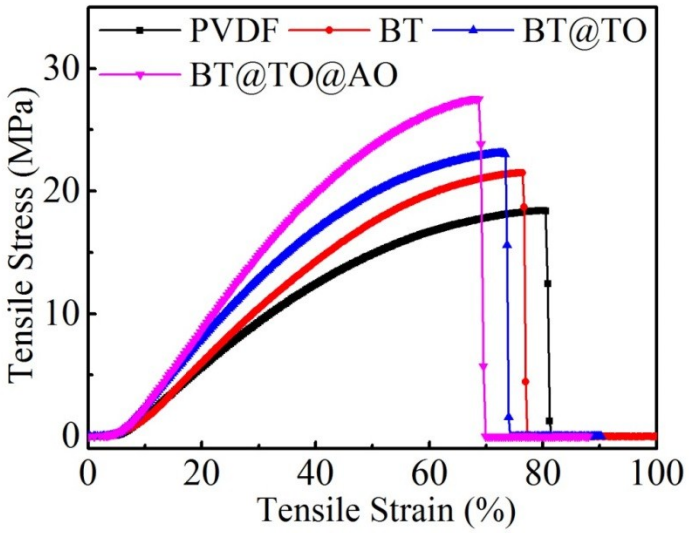

Figure S13 Tensile strain dependence of tensile stress of nanocompoaites loaded with 3.6 % BT NFs, BT@TO NFs, and BT@TO@AO NFs.